PHYSICAL REVIEW E **89**, 062316 (2014)

Clusters, asters, and collective oscillations in chemotactic colloids

Suropriya Saha,[1,2,*] Ramin Golestanian,[3,†] and Sriram Ramaswamy[2,1,‡]
[1] *Department of Physics, Indian Institute of Science, Bangalore 560 012, India*
[2] *TIFR Centre for Interdisciplinary Sciences, 21 Brundavan Colony, Osman Sagar Road, Narsingi, Hyderabad 500 075, India*
[3] *Rudolf Peierls Center for Theoretical Physics, University of Oxford, 1 Keble Road, Oxford OX1 3NP, United Kingdom*

(Received 30 March 2014; published 26 June 2014)

The creation of synthetic systems that emulate the defining properties of living matter, such as motility, gradient-sensing, signaling, and replication, is a grand challenge of biomimetics. Such imitations of life crucially contain active components that transform chemical energy into directed motion. These artificial realizations of motility point in the direction of a new paradigm in engineering, through the design of emergent behavior by manipulating properties at the scale of the individual components. Catalytic colloidal swimmers are a particularly promising example of such systems. Here we present a comprehensive theoretical description of gradient-sensing of an individual swimmer, leading controllably to chemotactic or anti-chemotactic behavior, and use it to construct a framework for studying their collective behavior. We find that both the positional and the orientational degrees of freedom of the active colloids can exhibit condensation, signaling formation of clusters and asters. The kinetics of catalysis introduces a natural control parameter for the range of the interaction mediated by the diffusing chemical species. For various regimes in parameter space in the long-ranged limit our system displays precise analogs to gravitational collapse, plasma oscillations, and electrostatic screening. We present prescriptions for how to tune the surface properties of the colloids during fabrication to achieve each type of behavior.

DOI: 10.1103/PhysRevE.89.062316 PACS number(s): 82.70.Dd, 05.65.+b, 47.57.J−

I. INTRODUCTION

Dynamic self-organization of motile components can be observed in a wide range of length scales, from bird flocks [1] to bacterial colonies [2,3] and assemblies of motor and structural proteins [4]. The fascination with these phenomena has naturally inspired researchers to use a physical understanding of motility to engineer complex emergent behaviors in model systems that promise revolutionary advances in technological applications if combined with other novel biomimetic functions, such as signal processing and decision making [5], or replication [6].

Symmetry-based phenomenological theories, coarse-grained or particle-based [7–13], offer a guide to the rich possibilities immanent in self-driven systems, but designing a system requires a bottom-up approach. Biological components pose inevitable limitations on this task, while chemical [14], mechanical [15], or externally actuated [16] imitations appear more promising. In addition to motility, living organisms have developed mechanisms that allow them to orient their motion in response to chemical gradients, and send signals to recruit or repel others [17]. Can inanimate matter imitate these more complex functions? We show that it can, and present the necessary design principles. We consider the case of catalytic active colloids [18–22], which we now describe in brief. Recall that a colloidal particle can be driven "phoretically" into motion by *externally imposed* chemical, electrostatic, or thermal gradients [23]. An *active* colloid—a particle coated asymmetrically with catalyst and immersed in a *uniform* background of substrate[1]—generates its own chemical gradient [18–22,24,25], and thus moves autonomously in a direction determined by the polarity of the coat (see Ref. [26] and references therein). Such self-phoretic particles, whose individual activity and interactions one can design, offer the opportunity to create systems with controllable, emergent collective behavior [27–37]. To this end it is essential to construct a description at a coarse-grained level, with coefficients expressed in terms of single-particle parameters.[2]

Our focus is on how the center of mass and orientation vector of an active colloid are affected by an externally imposed gradient of substrate molecules. Depending on details of geometry, activity, and mobility [25], an active colloid will respond to the local gradient of the substrate concentration through four distinct mechanisms. (i) *Chemotaxis:* The fluid flows set up around the particle can turn its axis of orientation to align parallel or antiparallel to the local gradient; this process has active contributions arising from the chemical reaction as well as passive ones. (ii) *Polar run-and-tumble motion:* The enzymatic rate depends nonlinearly on the local concentration of the substrate with a characteristic Michaelis-Menten form inherited from the underlying catalytic kinetics

---

[*] suropriya@physics.iisc.ernet.in
[†] ramin.golestanian@physics.ox.ac.uk
[‡] sriram@tifrh.res.in

[1] For consistency with the nomenclature of enzyme catalysis literature we refer to the reactant as 'substrate', not to be confused with other uses of the term.

[2] When this work was being prepared for submission, we learned of unpublished results from the groups of H. Stark and J. Brady on self-phoretic swimmers interacting through their diffusion fields. The construction of chemotactic behavior from the patterning of the colloid, the role of enzyme kinetics, the dynamics of orientation fields and aster formation, the occurrence of underdamped modes and the possibility of spontaneous oscillation are among the distinguishing features of our work.

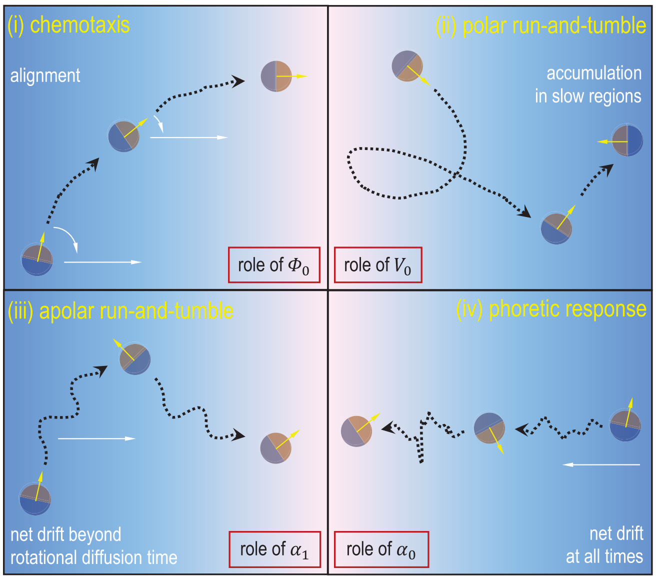

FIG. 1. (Color online) A schematic summary of the four different ways a single swimmer responds to gradients corresponding to the different terms in Eq. (1). In each panel, three consecutive snapshots (with equal time intervals) are sketched together with typical connecting trajectories. In (i) and (ii) the polarity of the colloid controls the direction of motion. In (iii) the motion will be along the main symmetry axis of the colloid but driven by the gradient (hence the colloid can move forward or backward instantaneously). In (iv) the motion is independent of the polarity and symmetry axis of the colloid. Processes (i) and (iv) represent steady angular and linear drift while in (ii) and (iii) the gradient-seeking behavior is assisted by noise. Each mechanism is controlled by the relevant spherical harmonics coefficient of the material-dependent particle mobility and activity, which can be modified by construction.

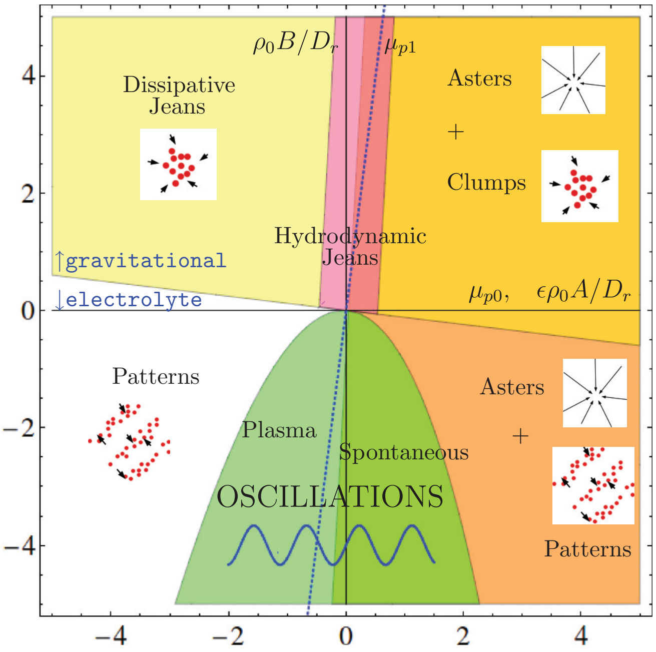

FIG. 2. (Color online) The phase diagram in the *reaction-limited* regime (with abundant fuel) shows a variety of possible states in the parameter space spanned by suitably non-dimensionalized effective chemotactic (A) and phoretic (B) response coefficients, defined in Eq. (9). The dashed line and the A-axes correspond to independent changes of the fundamental and first harmonic (μ_{p0} and μ_{p1}) of the mobility corresponding to the reaction product, respectively. They represent possible experimental paths that can be explored in sequences of experiments on particles designed with suitable mobility coats.

of the reactions [38]. The combination of enhanced activity at high concentrations and randomized orientation acts to effectively populate the colloids in "slow" regions [39]. (iii) *Apolar run-and-tumble motion:* An active colloid can also chemotax by a net motion of its center along a gradient in a noise-averaged sense. (iv) *Phoretic response:* The colloid moves along an external chemical gradient by diffusiophoresis. A summary of the different modes is depicted in Fig. 1.

Catalytic colloids consume a substrate and generate product molecules, and hence act as mobile sources and sinks of these chemicals in the solution making their concentration profile nonuniform. In a suspension of such active colloids, each individual responds—via the above four mechanisms—to the gradients produced by other colloids due to their activities. The various contributions are independent of each other and their balance will be modified as we move in the space of control parameters, leading to a variety of collective behaviors. In particular, we highlight the intriguing possibility that the positional and orientational degrees of freedom could exhibit different and independent types of order depending on the parameters, as shown in Figs. 2 and 3.

We consider a fluid medium containing a concentration $s(\mathbf{r},t)$ of substrate (S) molecules, which upon contact with a catalyst are converted to a product P with concentration $p(\mathbf{r},t)$. The rate of conversion κ obeys Michaelis-Menten kinetics [40], growing linearly at small s and crossing over to saturation for sufficiently large values of s. Our main results are as follows: **(1)** for the case of a uniform gradient of substrate, we establish the form of the angular velocity $\boldsymbol{\omega}$ induced on a single catalytic colloid as a function of the spherical harmonic components of the activity σ and the mobilities μ_s and μ_p corresponding to S and P. We can therefore propose criteria for the surface patterning required to produce chemotactic and anti-chemotactic motion. We also find the various contributions to the translational velocity $\boldsymbol{v}$ of the colloid, arising from self-propulsion and drift due to the external gradient. Explicitly, we find

$$\begin{aligned}\boldsymbol{\omega} &= \Phi_0(\sigma,\mu_p,\mu_s)\,\hat{\mathbf{n}}\times\nabla s,\\ \mathbf{v} &= V_0(s)\hat{\mathbf{n}} - \alpha_0\nabla s - \alpha_1\hat{\mathbf{n}}\hat{\mathbf{n}}\cdot\nabla s.\end{aligned} \tag{1}$$

where the definitions of the coefficients in terms of the surface properties of the colloids are given below. **(2)** We use our results for a single particle in an external gradient to construct the collective equations of motion for the number density and orientation of the colloids in a uniform medium, interacting via their effect on the substrate and product concentration fields. The interplay between self-propulsion, phoretic drift, and alignment, driven by and mediated via chemicals, falls into two distinct regimes. (a) When the fuel concentration is small enough such that the catalytic activity is *diffusion-limited*,

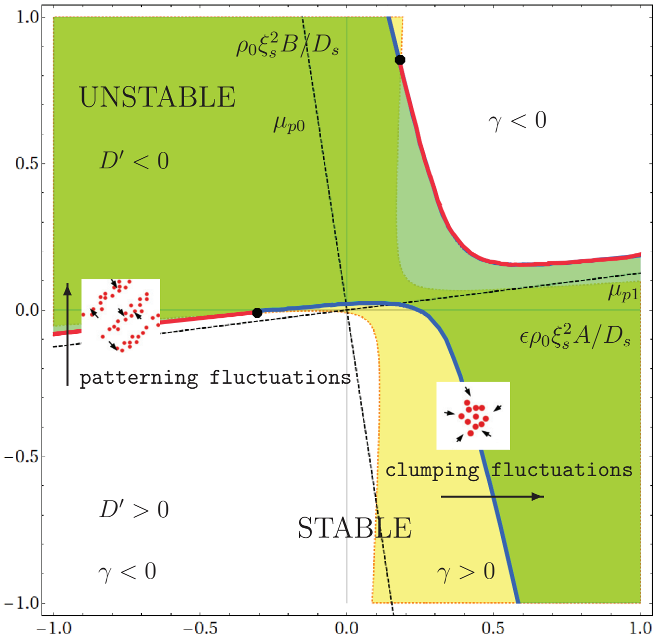

FIG. 3. (Color online) The *diffusion-limited* regime (with limited fuel supply) exhibits different types of instability in the parameter space spanned by suitably non-dimensionalized effective chemotactic (A) and phoretic (B) response coefficients, defined in Eq. (9). The effective diffusivity D' [defined in Eq. (11)] is negative in the green region and positive in the white or yellow regions, signaling the presence of an instability upon going from the yellow or white to green. The dominant fluctuations on approaching the instability signal a tendency to form modulations (across the red line) or clumps (across the blue line) state, depending on the sign of the parameter γ [defined in Eq. (12)]. The character of the fluctuations on the stability boundary changes at the location shown by the black dot. The axes corresponding to possible experimental changes of the fundamental and first harmonic (μ_{p0} and μ_{p1}) of the mobility corresponding to the reaction product, respectively, are shown by two dashed lines.

the chemical concentrations will be effectively screened, and the system could develop enhanced number fluctuations and clumping instabilities (where all wavelengths above a threshold are unstable) and patterns with a given length scale (where the fastest-growing mode has finite wavelength). (b) At sufficiently high fuel concentrations where the catalytic activity becomes *reaction-limited*, the chemical fields are not screened and can mediate long-ranged interactions that could lead to a wider variety of instabilities. In particular, for the case of effectively attractive phoretic interaction we observe collapse transitions that are dissipative analogs of a Jeans instability [42], with or without simultaneous condensation of asters. For effectively repulsive phoretic interactions, we observe counter-intuitively that a collapsed phase with aster condensation is still possible, as are stable phases exhibiting Debye-like screening, similar to electrolytes. Moreover, we find that in this regime the system could exhibit plasma-like oscillations in response to perturbations, or spontaneous, self-sustained ringing. Detailed phase diagrams inferred from our stability analysis and structure factor calculations are found in Figs. 2 and 3. These are parametrized, via definitions in Eq. (9) below, by coefficients A describing the chemotactic response from panels (i) and (ii) of Fig. 1, and B the phoretic response from panels (iii) and (iv) of that figure. We now show how we obtained these results.

A. Background: Diffusiophoresis and self-diffusiophoresis

Diffusiophoresis[3] is the force-free, torque-free propulsion of a colloid by a solute concentration gradient [23]. In a fluid of viscosity η at temperature T a species with concentration c interacting through an effective potential Ψ with a particle surface with normal along the local z axis gives rise, via the Stokes equation, to a surface "slip velocity" $\mathbf{v}_{\text{slip}} = \mu\nabla_{\|}c$, with the phoretic mobility $\mu = \frac{k_BT}{\eta}\int_0^\infty z(1-e^{-\Psi/k_BT})dz$ that can have either *sign* depending on Ψ. We are also interested here in *self*-diffusiophoresis [19] that occurs when ∇c is not imposed externally but generated by processes on the particle itself.

B. A single chemotactic motile colloid

Consider a single swimmer, whose mobilities and catalytic coat have the common symmetry axis $\hat{\mathbf{n}}$. When placed in a *uniform* substrate background, such a particle moves in a direction determined by $\hat{\mathbf{n}}$ if the coatings are sufficiently asymmetric [25]. What happens in an inhomogeneous background? Can the flows set up by the interaction of S and P with the swimmer surface reorient its axis $\hat{\mathbf{n}}$ with respect to the local concentration gradient, thus imitating chemotaxis? To answer this question, we solve for the concentrations s and p, with diffusivities D_s and D_p, respectively. We incorporate the catalytic chemical reaction S → P through source and sink boundary conditions on particle fluxes normal (⊥) to the swimmer surface:

$$-D_s\nabla_\perp s = -\kappa_1 s P_s\sigma(\theta,\phi); \quad -D_p\nabla_\perp p = \kappa_2 P_p\sigma(\theta,\phi), \tag{2}$$

where $P_p(\theta,\phi) \equiv 1 - P_s(\theta,\phi)$ is the probability that the enzyme at (θ,ϕ) is bound to the substrate. Stationarity implies $\kappa_1 s P_s = \kappa_2 P_p$ leading to the Michaelis-Menten [40] expression $\kappa_2 P_p \equiv \kappa(s) \equiv \kappa_2\kappa_1 s/(\kappa_2+\kappa_1 s)$ for the reaction velocity per molecule. Number conservation for the products and substrates, and the assumption that s and p diffuse rapidly compared to the colloid so that time dependencies and advection by flow [41] can be ignored give $D_p p + D_s s = D_s s_b$, where s_b is the background substrate profile. We thus need to solve for just one of the two concentration fields. We work in the linear regime[4] $s_b \ll \kappa_1/\kappa_2$, where the profile of product p resulting from this process is sensitive to the imposed gradient of s, and in the limit where S diffuses rapidly so that its profile is maintained. The resulting slip velocity, which has contributions from both the substrate and the product, leads to the linear and angular velocities $\boldsymbol{\omega} = -\frac{3}{16\pi R}\int \hat{\mathbf{r}} \times \mathbf{v}_{\text{slip}}(\mathbf{r})\, d\Omega$ and $\mathbf{v} = -\frac{1}{4\pi}\int \mathbf{v}_{\text{slip}}(\mathbf{r})\, d\Omega$ for spherical colloids.

---

[3] We will not discuss similar phoretic propulsion mechanisms through gradients in temperature or electrostatic potentials.

[4] Results from another limit of interest, $D_p \gg D_s$ and $s_b \ll \kappa_1/\kappa_2$, in which the chemical reaction influences significantly the local value of s so that the coupled dynamics of orientation and translation can lead to oscillations, will be discussed elsewhere.

To understand the general trends in chemotactic behavior arising from simple catalytic patterns, we work with a limited number of non-zero spherical harmonic components of σ and μ_p. For example, taking $\sigma_l, \mu_{pl} = 0$ for $l \geqslant 3$ we find the expression for the angular velocity given in Eq. (1) with

$$\Phi_0 = -\frac{3\mu_{s1}}{4R} - \frac{\kappa_1}{60D_p}\left(5\mu_{p1}\sigma_0 + 2\mu_{p2}\sigma_1 - \mu_{p1}\sigma_2\right), \tag{3}$$

where a negative (positive) value corresponds to chemotactic (anti-chemotactic) response. The first term on the left is the passive response to the external gradient due to a polarity in μ_s alone while the second term is the active contribution involving both σ and μ_p. The form of Eq. (3) serves to illustrate some features that hold even without the truncated expansion in l: if either σ or μ_p contain all odd or all even harmonics there is no reorientation in response to the gradient, a result which holds for spheroidal swimmers as well. The expression for the product contribution in Eq. (3) is a sum of products of σ_l and $\mu_{p,l\pm1}$, which can be used to design chemotactic colloids with a desired response. Lastly, regardless of the form of σ, $\omega = 0$ for μ_p uniform over the sphere.

We also obtain the net translational velocity $\mathbf{v}$, as in Eq. (1) where

$$\begin{aligned} V_0 &= \frac{\kappa_1 s_b}{15D_p}(5\sigma_1\mu_{p0} + 2\sigma_2\mu_{p1} - \sigma_1\mu_{p2}),\\ \alpha_0 &= -\left(\mu_{s0} + \frac{1}{10}\mu_{s2}\right) - \frac{\kappa_1 R}{10D_p}\left(\sigma_0\mu_{p2} - \frac{2}{9}\sigma_1\mu_{p1}\right.\\ &\quad \left. - 2\sigma_2\mu_{p0} + \frac{1}{35}\sigma_2\mu_{p2}\right),\\ \alpha_1 &= -\frac{1}{10}\mu_{s2} - \frac{\kappa_1 R}{30D_p}\left(10\sigma_0\mu_{p0} + \sigma_0\mu_{p2} + 2\sigma_1\mu_{p1}\right.\\ &\quad \left. - 2\sigma_2\mu_{p0} + \frac{29}{35}\sigma_2\mu_{p2}\right). \end{aligned} \tag{4}$$

The three contributions to the translational velocity correspond to self-propulsion (along $\hat{\mathbf{n}}$), phoretic drift (along ∇s), and an anisotropic drift that is instantaneously along $\hat{\mathbf{n}}$, but leads to net motion along ∇s as rotational noise decorrelates $\hat{\mathbf{n}}$. The latter amounts to a contribution to run-and-tumble gradient-seeking motion, which we name apolar run-and-tumble; see Fig. 1.

To demonstrate how the chemotactic response of catalytic colloids can be designed, we have calculated Φ_0 for an example of swimmers with uniform spheroidal caps of catalytic and mobility patterns as $\sigma(\theta) \propto \Theta(\theta - \theta_1)$ and $\mu_p \propto 1 + \Theta(\theta - \theta_2)$. Figure 4 shows Φ_0 as a function of θ_1 for different values of θ_2. For $\theta_2 = \pi/2$, Φ_0 is antisymmetric as a function of θ_1. For a given θ_2, Φ_0 peaks near $\theta_1 = \theta_2$ as the slip velocity is maximum when the position where μ_p is maximum coincides with the region where p changes most rapidly, which for the given form of σ is at θ_1. This example showcases the possibility to control the response of individual catalytic colloids, and thus their collective behaviors, by following design rules that include varying systematically their geometric features. We now combine the individual responses of active colloids to construct a theoretical description for their collective behaviors.

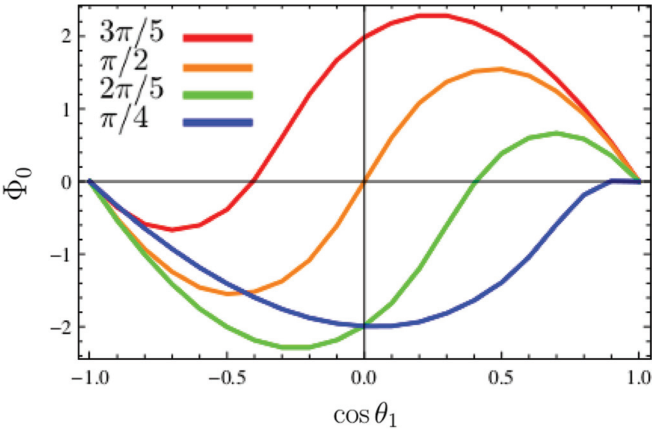

FIG. 4. (Color online) Angular velocity coefficient for spherical colloids as a function of θ_1 (that parametrizes the size of the catalytic coating) for different values of θ_2 (that parametrizes the mobility pattern) quoted in the legend.

II. FROM CHEMOTAXIS TO COLLECTIVE MOTION

Catalytic swimmers of the type discussed above interact through the S and P chemical fields as well as via hydrodynamics [43,44]. We restrict our attention to their chemotactic interaction, and construct the collective behavior of many swimmers by looking at pairwise interactions. Consider, therefore, two swimmers separated by a distance r in a uniform medium of substrate molecules. The reaction S → P that takes place on the surface of each swimmer modifies the s field as seen by the others, and each is also a source for P. In the absence of a background of other swimmers, inhomogeneities in the s and p fields in steady state decay as $1/r$. Each swimmer senses and responds to the magnitude and the gradient of s through the motility and chemotaxis mechanisms outlined above. In addition, each particle responds to the p field produced by the reactions on the surfaces of all the particles, just as it would to any externally imposed solute gradient [23]. The resulting equations of motion for the position $\mathbf{r}_\alpha$ and orientation unit vector $\hat{\mathbf{n}}_\alpha$ of the αth, to linear order in ∇s, ∇p, take the form

$$\begin{aligned} \frac{d\mathbf{r}_\alpha}{dt} &= V_0(s)\hat{\mathbf{n}}_\alpha - \alpha_0\nabla s - \alpha_1\hat{\mathbf{n}}_\alpha\hat{\mathbf{n}}_\alpha\cdot\nabla s + \beta_0\nabla p\\ &\quad + \beta_1\hat{\mathbf{n}}_\alpha\hat{\mathbf{n}}_\alpha\cdot\nabla p + \sqrt{2D}\,\mathbf{f}^r_\alpha(t),\\ \frac{d\mathbf{n}_\alpha}{dt} &= \Phi_0(\hat{\mathbf{n}}_\alpha \times \nabla s)\times\hat{\mathbf{n}}_\alpha + \Omega_0(\hat{\mathbf{n}}_\alpha\times\nabla p)\times\hat{\mathbf{n}}_\alpha\\ &\quad + \sqrt{2D_r}\,\hat{\mathbf{n}}_\alpha\times\mathbf{f}^n_\alpha(t), \end{aligned} \tag{5}$$

where additional coupling constants

$$\Omega_0 = -\frac{3\mu_{p1}}{4R}, \quad \beta_0 = -\left(\mu_{p0} + \frac{1}{10}\mu_{p2}\right), \quad \beta_1 = -\frac{1}{10}\mu_{p2}, \tag{6}$$

are introduced to take account of the response of each colloid to a product gradient produced by the others. In Eq. (5) thermal as well as active fluctuations are included phenomenologically via Gaussian unit-strength white noise terms $\mathbf{f}^r_\alpha, \mathbf{f}^n_\alpha$, with strengths D and D_r. $\Phi_0 > 0$ and $\Omega_0 > 0$ correspond to swimmers that respond chemotactically to ∇s and ∇p

respectively. $\alpha_0 > 0$ and $\beta_0 > 0$ imply attractive contributions to the interactions between the swimmers due to s and p, respectively. $V_0(s) > 0$ by definition as we choose $\hat{\mathbf{n}}_\alpha$ to point in the direction in which a solitary swimmer moves. The form of Eq. (5) follows on the general grounds of symmetry. The point of our calculation is that it gives explicit expressions for the tactic and phoretic mobilities and the expressions for α_i and β_i. Moreover, the substrate and product fields are themselves determined by the distribution of colloid positions and orientations. The substrate is consumed and the product is generated at the rate $Q(\mathbf{r},t) = \kappa(s)\sum_\alpha \int_{|\mathbf{X}_\alpha|=R} \delta(\mathbf{r} - \mathbf{r}_\alpha - \mathbf{X}_\alpha)\sigma(\mathbf{X}_\alpha \cdot \hat{\mathbf{n}}_\alpha)$, where $\mathbf{X}_\alpha$ is the position coordinate on the αth swimming sphere of radius R, and the catalytic coat σ is expressed in laboratory-frame coordinates. We assume the system is maintained[5] in a steady state with mean substrate concentration s_0 and develop Q to leading orders in a gradient expansion to obtain a coarse-grained description. We begin by relating the s and p fields to the coarse-grained density and orientation fields of the colloids, namely, $\sum_\alpha \delta(\mathbf{r} - \mathbf{r}_\alpha) = \rho(\mathbf{r})$ and $\sum_\alpha \hat{\mathbf{n}}_\alpha \delta(\mathbf{r} - \mathbf{r}_\alpha) = \mathbf{w}(\mathbf{r})$ (see the Supplemental Material [45]). We find

$$\left(\partial_t - D_s\nabla^2\right)s = -N\kappa(s)(\rho - \epsilon\nabla\cdot\mathbf{w}) = -\left(\partial_t - D_p\nabla^2\right)p. \tag{7}$$

In Eq. (7), $N = 4\pi R^2\sigma_0$ is the total number of enzymatic sites on the surface of the swimmer and $\epsilon = R\sigma_1/3\sigma_0$ measures the degree of polarity of the catalytic coat. We work in the limit of $\partial_t s = \partial_t p = 0$. Linearizing Eq. (7) around a steady state with (ρ_0, s_0, p_0), we find the following results for the Fourier components of the concentration at wave vector $\mathbf{q}$: $s_\mathbf{q} = -N\kappa(s_0)(\rho_\mathbf{q} - \epsilon i\mathbf{q}\cdot\mathbf{w}_\mathbf{q})/[D_s(q^2 + \xi_s^{-2})]$, $p_\mathbf{q} = -D_s s_\mathbf{q}/D_p$, where we introduce *the screening length*

$$\xi_s = [N\rho_0\kappa'(s_0)/D_s]^{-1/2}, \tag{8}$$

that is a measure of the range of interactions mediated by S and P. For $s_0 \ll \kappa_2/\kappa_1$, i.e., on the linear or *unsaturated* part of the MM curve, ξ_s is finite and the interactions are therefore short-ranged. For $s_0 \gg \kappa_2/\kappa_1$, i.e., on the *saturated* part of the MM curve, $\xi_s \to \infty$ and the product mediates an effective long-ranged interaction amongst the colloids.

Starting from the Langevin equations in Eq. (5), we next construct equations of motion for ρ and $\mathbf{n}(\mathbf{r}) = \mathbf{w}/\rho$ as defined above Eq. (7). While coarse-graining, we see inevitably that the dynamical equation for $\mathbf{n}$ involves higher moments of the orientational distribution function, which must be re-expressed in terms of lower moments [46,47] using an appropriate closure which we discuss in the Supplemental Material [45]. The S and P fields produced by inhomogeneities in density and the divergence of the polar order parameter mediate interactions between swimmers through ρ and the longitudinal component $\mathbf{n}_{Lq} = \hat{\mathbf{q}}\hat{\mathbf{q}}\cdot\mathbf{n}_q$. The linearized dynamics in the isotropic phase closes in terms ρ and $\mathbf{n}_{L\mathbf{q}}$, whose coarse-grained equations we present in the saturated limit and for wave numbers $q \ll \xi_s^{-1}$ in the unsaturated case. We will see that despite the presence of a self-propelled velocity field and a density, there is an important contrast relative to models such as Toner-Tu [7]: the interactions considered here offer no mechanism to promote flocking, i.e., the global parallel alignment of $\mathbf{n}$.

We have calculated the mode structure and steady state structure factors $S_\rho = \int_\omega \langle|\rho_{\mathbf{q}\omega}|^2\rangle$ and $S_n = \int_\omega \langle|\mathbf{n}_{L\mathbf{q}\omega}|^2\rangle$ for both the unsaturated and the saturated cases by adding phenomenological gaussian white noise terms, conserving for ρ and nonconserving for $\mathbf{n}_L$, to the equations of motion. The equations of motion and their stability analysis which we now present are best shown in terms of coefficients

$$\begin{aligned} A &= N\kappa(s_0)\left[\frac{\Omega_0}{D_p} - \frac{\Phi_0}{D_s} + \frac{V_0(s_0)}{2D_s}\frac{d\ln\kappa}{ds}\Big|_{s_0}\right], \\ B &= N\kappa(s_0)\left[\frac{1}{D_p}\left(\beta_0 + \frac{\beta_1}{3}\right) + \frac{1}{D_s}\left(\alpha_0 + \frac{\alpha_1}{3}\right)\right], \end{aligned} \tag{9}$$

which give the effective chemotactic and phoretic response to gradients, respectively.

III. UNSATURATED

In the unsaturated case $\xi_s < \infty$, for wave numbers $q \ll \xi_s^{-1}$, coarse grained equations read

$$\left[\partial_t + 2D_r - \left(D + \frac{v_1^2 s_0^2}{30D_r}\right)\nabla^2 + \left(\epsilon\rho_0\xi_s^2 A - \frac{v_1^2 s_0^2}{90D_r}\right)\right.$$
$$\left.\times\,\nabla\nabla\cdot\right]\mathbf{n}_L + \frac{\left(v_1 s_0 - \rho_0\xi_s^2 A\right)}{3\rho_0}\nabla\rho = 0, \tag{10a}$$

$$\left[\partial_t - \left(D - \rho_0\xi_s^2 B\right)\nabla^2\right]\rho_0^{-1}\delta\rho + \left(v_1 s_0 - \epsilon\rho_0\xi_s^2 B\nabla^2\right)$$
$$\times\,\nabla\cdot\mathbf{n}_L = 0, \tag{10b}$$

where we use $V_0(s_0) \equiv v_1 s_0$ as the self-phoretic velocity scales linearly with the substrate concentration.

Several features of Eq. (10) are noteworthy. From Eq. (7), P is abundantly available or S is depleted where the density ρ is high. Phoretic movement up (down) the gradient of $p\,(s)$ can thus lead to a propensity of swimmers to swim up their concentration gradients and hence a change in the sign of the diffusivity in Eq. (10b) through $\rho_0\xi_s^2 B$. Since the swimmer preferentially moves along its polar axis, $\mathbf{n}$ can be viewed as a velocity field, and the $\nabla\rho$ term as a pressure gradient. We see that for large enough $\epsilon\rho_0\xi_s^2 A$, the signs of coefficients that are analogous to bulk viscosity, and squared sound speed can change signaling an instability and possible novel condensation phenomena whose nature will be revealed only by a nonlinear treatment with appropriate noise terms. Note that A contains two contributions: (i) chemotactic alignment with the local gradient in s and p and (ii) slowing down of swimmers due to increased substrate consumption as a result of a local excess of ρ that depletes s locally. This provides a realization of the density-dependent self-propulsion velocity of [48]. In the overdamped limit, for large A and B, one eigenmode with relaxation

$$-i\omega = -D'q^2 \equiv -\left(D + \frac{v_1^2 s_0^2}{6D_r} - \rho_0\xi_s^2 B - \frac{v_1 s_0\rho_0\xi_s^2 A}{6D_r}\right)q^2 \tag{11}$$

---

[5] We assume prompt replenishment of consumed substrate, and we work on timescales long enough that the product has reached the sample boundaries, where it is absorbed.

goes unstable with growth rate $\sim q^2$ at small q. Competition with stabilizing effects at larger q will lead to a modulated growth morphology with a length scale determined by the wave number of peak growth $\sim |D'|^{1/2}$. The other mode, controlled by D_r, remains stable for $q \to 0$, i.e., interactions do not promote flocking. Working at large D_r also justifies the overdamped limit.

In the parameter range where these modes are stable, the steady-state static small-q structure factor takes the form $S_\rho \propto 1/(D' + \gamma q^2)$, where

$$\begin{aligned}\gamma = 2\xi_s^2 D_r\bigg[&\rho_0\xi_s^2 B + \frac{\rho_0\xi_s^2 A v_1 s_0}{6D_r} + \frac{1}{3}\epsilon\rho_0\xi_s^2 B\big(v_1 s_0 - \rho_0\xi_s^2 A\big) \\ &+ \big(D - \epsilon\rho_0\xi_s^2 A\big)\bigg(D + \frac{2v_1^2 s_0^2}{45 D_r} - \rho_0\xi_s^2 B\bigg) \\ &+ D'\big(\rho_0\xi_s^2 B + \epsilon\rho_0\xi_s^2 A - 2D\big)\bigg]. \end{aligned} \tag{12}$$

For $\gamma > 0$, as $D' \to 0^+$, S_ρ displays fluctuations with a correlation length $\sqrt{\gamma/D'}$ that diverges as $D' \to 0$, presaging the onset of clumping (see Fig. 3). Still in the linearly stable regime but with $\gamma < 0$, an analysis to order q^4 shows that the system has a tendency towards patterning with a characteristic length scale $\sim |\gamma|^{-1/2}$, whose origin involves a competition between the chemotactic (A) and phoretic (B) response to gradients.

IV. SATURATED

Next we consider the saturated limit $\xi_s \to \infty$, realized by working at saturation concentrations on the MM curve. It is useful to define $\mathbf{E}(\mathbf{r}) = -\boldsymbol{\nabla}\int_{\mathbf{r}'}\rho(\mathbf{r}')/|\mathbf{r}-\mathbf{r}'|$, which plays the role of an electric field in Eq. (13a) below. Equation (7) then implies $\boldsymbol{\nabla} s = N\kappa_2(\mathbf{E} - \epsilon\rho_0\mathbf{n}_L)/D_s$. In this limit the orientation and density fields satisfy[6]

$$\begin{aligned}\bigg[\partial_t - \bigg(D + \frac{v_0^2}{30D_r}\bigg)\nabla^2\bigg]\mathbf{n}_L + \frac{v_0}{3\rho_0}\boldsymbol{\nabla}\rho + \frac{A}{3}\mathbf{E} \\ - \bigg[\frac{v_0^2}{90D_r} - \frac{2\epsilon N\kappa_2 v_0\rho_0}{135 D_r}\bigg(\frac{\beta_1}{D_p} + \frac{\alpha_1}{D_s}\bigg)\bigg]\boldsymbol{\nabla}\boldsymbol{\nabla}\cdot\mathbf{n}_L \\ + \bigg[\frac{2\epsilon^2 A^2\rho_0^2}{15D_r}n_L^2 - \frac{\epsilon A}{3}\rho_0 + 2D_r\bigg]\mathbf{n}_L = 0,\end{aligned} \tag{13a}$$

$$(\partial_t - D\nabla^2)\rho + \rho_0(v_0 + \epsilon\rho_0 B)\boldsymbol{\nabla}\cdot\mathbf{n}_L - \rho_0 B\boldsymbol{\nabla}\cdot\mathbf{E} = 0, \tag{13b}$$

where $v_0 \equiv \lim_{s_0 \gg \kappa_2/\kappa_1} V_0(s_0)$. The electric-field character of $\mathbf{E}$ is evident in Eq. (13a) through the alignment term $\propto A$ and the Ohmic current $\propto B$ in Eq. (13b). Note that a large and positive $\epsilon\rho_0 A/3$ can destabilize the $n_L = 0$ state leading—once higher order terms are taken into account—to a state of nonzero $\mathbf{n}_L$, i.e., a condensation of asters. The phenomenon is related to that reported in [49], with the important difference in our case of long-range interactions mediated by $\mathbf{E}$, as in [50], with a resemblance to gravitational collapse [42].

In the overdamped limit, i.e., for sufficiently large D_r, the relaxation rates of the eigenmodes are

$$-i\omega = \begin{cases} \frac{G}{2D_r'} - \big[2D + \frac{v_0(v_0+\epsilon\rho_0 B)}{3D_r'}\big]q^2, \\ -2D_r' + O(q^2), \end{cases} \tag{14}$$

where $D_r' = D_r - \epsilon\rho_0 A/6$ represents a modified rotational diffusion, and $G = 2\rho_0 B D_r + \frac{1}{3}\rho_0 A v_0$ is an effective control parameter for the nature of interaction between the swimmers. Equation (13) shows that in the saturated limit the effective long-ranged interaction between colloids (as mediated by S and P) leads to non-vanishing relaxation rates at $q = 0$ for both modes, notwithstanding the conservation law governing ρ.

For $G < 0$, the swimmers interact with long-ranged repulsive interactions. The structure factor $S_\rho(q \to 0) = 0$, as it is a ratio of the strength of fluctuations and the wave number independent relaxation rate, which is reminiscent of suppression of charge density fluctuations in electrolytes. Including terms of higher order in q yields a density structure factor with a peak at $q \sim G^{1/4}$, which is characteristic of microphase separation (white region in Fig. 2). We see from Eq. (13) that for $G > 0$ and large D_r' the isotropic state with uniform density is linearly unstable for small wave number q, including $q = 0$. This effect is a dissipative analog of the gravitational Jeans instability [42], and is a consequence of the long-ranged attractive interaction (yellow). Related behavior has been predicted for thermophoretic colloids [50]. Letting $D_r' \to 0$ by increasing A and keeping $G > 0$ brings the system out of the overdamped region where the relaxation of $\mathbf{n}$ slows down and it behaves like a velocity field. This behavior where the system resembles a gravitational system conserving momentum and displays an instability formally equivalent to the standard hydrodynamic Jeans instability [42] (magenta). Modes with wave numbers larger than a crossover scale given by a competition between the interaction strength G and a squared sound speed equivalent $v_0(v_0 + \epsilon\rho_0 B)$ for our system are oscillatory, whereas modes with smaller wave numbers are too "massive" and collapse. On further tuning the parameters to approach $D_r' < 0$, notwithstanding the value of G, one anticipates an instability towards a spontaneously oscillating state (green). Restricting our attention to the stable case, we find a structure factor for $\mathbf{n}_L$ with a correlation length $\sim (D/D_r')^{1/2}$ that grows as D_r' decreases, indicating strong fluctuations towards aster formation. For small D_r' and $G < 0$ the response shows "plasma oscillations" [51] with frequency $\sim \sqrt{|G|}$. For $D_r' < 0$ (dark green), the system can also develop spontaneous oscillations, or ringing.

V. SUMMARY

A colloid patterned with catalyst and immersed in a maintained reactant medium is a minimal nonequilibrium particle, displaying directed motion and related behaviors ruled out at thermal equilibrium. We have determined theoretically the nature of patterning that will cause such an active colloid to reorient along and move up or down a gradient of chemical reactant, thus delineating the principles for the design of chemotactic self-phoretic particles. Coarse-graining the resulting Langevin equations for the position and polar

---

[6] In Eq. (10) we have displayed only those nonlinear terms required to stabilized a state of nonzero $\mathbf{n}_L$. The complete equations may be seen in the Supplemental Material [45].

axis of one particle, we discover the dynamics of the density and polar order parameter of a collection. The interplay of chemotaxis and phoresis leads to clumping and patterning at low reactant concentration; at high concentration, the slow decay of diffusing reactants and products yields analogues of electrostatic and gravitational phenomena—Debye screening, microphase separation, plasma oscillations and gravitational collapse. The interactions promote aster formation, not a flocking transition, and the instabilities mediated by the long-range diffusion fields have a character distinct from those the generic instability driven by the velocity field in Stokesian active liquid crystals. We look forward to experimental tests and, eventually, practical application of our predictions.

ACKNOWLEDGMENTS

R.G. and S.R. acknowledge HFSP Grant No. RGP0061/2013 and a J. C. Bose Fellowship, respectively, and both thank the Isaac Newton Institute for Mathematical Sciences where a part of this work was completed.

[1] A. Cavagna and I. Giardina, Annu. Rev. Condens. Matt. Phys. **5**, 183 (2014).
[2] E. Ben-Jacob, I. Cohen, and H. Levine, Adv. Phys. **49**, 395 (2000).
[3] H. P. Zhang, A. Be'er, E. L. Florin, and H. L. Swinney, PNAS **107**, 13626 (2010).
[4] F. Schweitzer, *Brownian Agents and Active Particles: Collective Dynamics in the Natural and Social Sciences (Springer Series in Synergetics)* (Springer, Berlin, 2007).
[5] The SWARMS project webpage: www.swarms.org.
[6] T. Wang *et al.*, Nature **478**, 225 (2011).
[7] J. Toner and Y. Tu, Phys. Rev. E **58**, 4828 (1998).
[8] S. Ramaswamy, Annu. Rev. Condens. Matt. Phys. **1**, 323 (2010).
[9] M. C. Marchetti, Rev. Mod. Phys. **85**, 1143 (2013).
[10] G. Grégoire and H. Chaté, Phys. Rev. Lett. **92**, 025702 (2004).
[11] T. Vicsek and A. Zafeiris, Phys. Rep. **517**, 71 (2012).
[12] A. W. C. Lau and T. C. Lubensky, Phys. Rev. E **80**, 011917 (2009).
[13] J. Bialké, H. Löwen, and T. Speck, Europhys. Lett. **103**, 30008 (2013).
[14] S. Thutupalli, R. Seemann, and S. Herminghaus, New J. Phys. **13**, 073021 (2011).
[15] D. Yamada, T. Hondou, and M. Sano, Phys. Rev. E **67**, 040301 (2003).
[16] A. Ghosh and P. Fischer, Nano Lett. **9**, 2243 (2009).
[17] E. F. Keller and L. A. Segel, J. Theor. Biol. **30**, 235 (1971).
[18] W. F. Paxton *et al.*, J. Am. Chem. Soc. **126**, 13424 (2004).
[19] R. Golestanian, T. B. Liverpool, and A. Ajdari, Phys. Rev. Lett. **94**, 220801 (2005).
[20] J. R. Howse, R. A. L. Jones, A. J. Ryan, T. Gough, R. Vafabakhsh, and R. Golestanian, Phys. Rev. Lett. **99**, 048102 (2007).
[21] H. Ke, S. Ye, R. L. Carroll, and K. Showalter, J. Phys. Chem. A **114**, 5462 (2010).
[22] H. R. Jiang, N. Yoshinaga, and M. Sano, Phys. Rev. Lett. **105**, 268302 (2010).
[23] J. L. Anderson, Annu. Rev. Fluid. Mech. **21**, 61 (1988).
[24] G. Rückner and R. Kapral, Phys. Rev. Lett. **98**, 150603 (2007).
[25] R. Golestanian, T. B. Liverpool, and A. Ajdari, New J. Phys. **9**, 126 (2007).
[26] P. E. Lammert, J. Prost, and R. Bruinsma, J. Theor. Biol. **178**, 387 (1996).
[27] Y. Hong, N. M. K. Blackman, N. D. Kopp, A. Sen, and D. Velegol, Phys. Rev. Lett. **99**, 178103 (2007).
[28] R. Golestanian, Phys. Rev. Lett. **102**, 188305 (2009).
[29] M. E. Ibele, T. E. Mallouk, and A. Sen, ACS Nano. **8**, 4845 (2010).
[30] D. Kagan, S. Balasubramanian, and J. Wang, Angew. Chem. Int. Ed. **50**, 503 (2011).
[31] I. Theurkauff, C. Cottin-Bizonne, J. Palacci, C. Ybert C, and L. Bocquet, Phys. Rev. Lett. **108**, 268303 (2012).
[32] J. Palacci, S. Sacanna, A. P. Steinberg, D. J. Pine, and P. M. Chaikin, Science **339**, 936 (2013).
[33] W. Duan, R. Liu, and A. Sen, J. Am. Chem. Soc. **135**, 1280 (2013).
[34] G. Volpe *et al.*, Soft Matter **7**, 8810 (2011).
[35] F. Kümmel, Phys. Rev. Lett. **110**, 198302 (2013).
[36] M. N. Popescu *et al.*, Eur. Phys. J. E **31**, 351 (2010).
[37] L. Baraban, S. M. Harazim, S. Sanchez, and O. G. Schmidt, Angew. Chem. Int. Ed. **52**, 5552 (2013).
[38] S. Ebbens, M.-H. Tu, J. R. Howse, and R. Golestanian, Phys. Rev. E **85**, 020401(R) (2012).
[39] M. E. Cates and J. Tailleur, Europhys. Lett. **101**, 20010 (2013).
[40] P. C. Nelson, *Biological Physics* (WH Freeman, New York, 2007).
[41] G. P. Alexander and A. J. Liu, arXiv:1107.3851.
[42] J. Jeans, *Astronomy and Cosmogony*, 2nd ed. (Cambridge University Press, Cambridge, 1929).
[43] E. Lushi, R. E. Goldstein, and M. J. Shelley, Phys. Rev. E **86**, 040902(R) (2012).
[44] A. Zöttl and H. Stark, Phys. Rev. Lett. **112**, 118101 (2014).
[45] See Supplemental Material at http://link.aps.org/supplemental/10.1103/PhysRevE.89.062316 for details on the derivation.
[46] E. Bertin, M. Droz, and G. Grégoire, Phys. Rev. E **74**, 022101 (2006).
[47] D. Saintillan and M. J. Shelley, Phys. Fluids **20**, 123304 (2008).
[48] Y. Fily and M. C. Marchetti, Phys. Rev. Lett. **108**, 235702 (2012).
[49] K. Gowrishankar and M. Rao, arXiv:1201.3938v1.
[50] R. Golestanian, Phys. Rev. Lett. **108**, 038303 (2012).
[51] L. Tonks and I. Langmuir, Phys. Rev. **33**, 195 (1929).